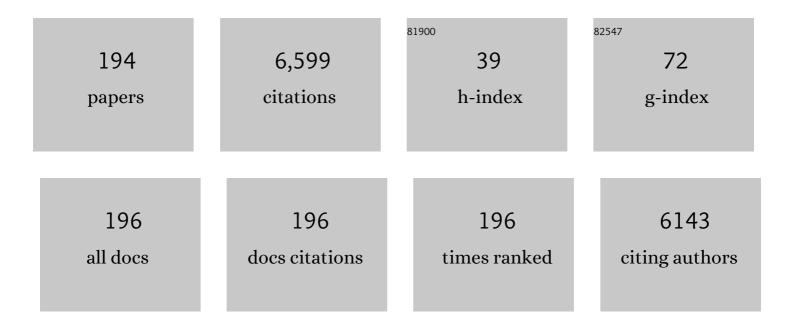
List of Publications by Year in descending order

Source: https://exaly.com/author-pdf/48289/publications.pdf Version: 2024-02-01



#	Article	IF	CITATIONS
1	The molecular representations of coal – A review. Fuel, 2012, 96, 1-14.	6.4	550
2	CO <sub>2</sub> Adsorption-Based Separation by Metal Organic Framework (Cu-BTC) versus Zeolite (13X). Energy & Fuels, 2009, 23, 2785-2789.	5.1	397
3	CO2 capture by adsorption: Materials and process development. International Journal of Greenhouse Gas Control, 2007, 1, 11-18.	4.6	363
4	Aminopropyl-functionalized mesoporous silicas as CO2 adsorbents. Fuel Processing Technology, 2005, 86, 1435-1448.	7.2	311
5	Diethylenetriamine[propyl(silyl)]-Functionalized (DT) Mesoporous Silicas as CO2Adsorbents. Industrial & Engineering Chemistry Research, 2006, 45, 2626-2633.	3.7	233
6	The utility of coal molecular models. Fuel Processing Technology, 2011, 92, 718-728.	7.2	181
7	The transformation of kaolin to low-silica X zeolite. Zeolites, 1997, 19, 359-365.	0.5	133
8	Advanced adsorbents based on MgO and K2CO3 for capture of CO2 at elevated temperatures. International Journal of Greenhouse Gas Control, 2011, 5, 634-639.	4.6	126
9	Polycyclic aromatic hydrocarbons in Australian coals. I. Angularly fused pentacyclic tri- and tetraaromatic components of Victorian brown coal. Geochimica Et Cosmochimica Acta, 1983, 47, 2141-2155.	3.9	124
10	Preparation and characterization of mesoporous silica supported cobalt oxide as a catalyst for the oxidation of cyclohexanol. Journal of Molecular Catalysis A, 2012, 358, 79-88.	4.8	112
11	Ewald Summation for Molecular Simulations. Journal of Chemical Theory and Computation, 2015, 11, 3684-3695.	5.3	108
12	Mechanical/thermal dewatering of lignite. Part 3: Physical properties and pore structure of MTE product coals. Fuel, 2007, 86, 3-16.	6.4	105
13	CO2 adsorption, selectivity and water tolerance of pillared-layer metal organic frameworks. Microporous and Mesoporous Materials, 2010, 132, 305-310.	4.4	103
14	Stepwise growth of melamine-based dendrimers into mesopores and their CO2 adsorption properties. Microporous and Mesoporous Materials, 2008, 111, 536-543.	4.4	101
15	Physico-chemical properties of Loy Yang lignite dewatered by mechanical thermal expression. Fuel, 2005, 84, 1940-1948.	6.4	96
16	Hydrothermal dewatering of a Chinese lignite and properties of the solid products. Fuel, 2016, 180, 473-480.	6.4	94
17	Amine modified mesocellular siliceous foam (MCF) as a sorbent for CO2. Chemical Engineering Research and Design, 2011, 89, 1647-1657.	5.6	79
18	Polycyclic aromatic hydrocarbons in Australian coals II. Novel tetracyclic components from Victorian brown coal. Geochimica Et Cosmochimica Acta, 1984, 48, 2037-2043.	3.9	75

#	Article	IF	CITATIONS
19	CO2 adsorption by amine modified siliceous mesostructured cellular foam (MCF) in humidified gas. Microporous and Mesoporous Materials, 2014, 186, 84-93.	4.4	71
20	Polycyclic aromatic hydrocarbons in Australian coals—III. Structural elucidation by proton nuclear magnetic resonance spectroscopy. Organic Geochemistry, 1988, 12, 261-271.	1.8	70
21	Comparison of Cu-BTC and zeolite 13X for adsorbent based CO2 separation. Energy Procedia, 2009, 1, 1265-1271.	1.8	67
22	Characterisation of lignite as an industrial adsorbent. Fuel, 2011, 90, 1567-1574.	6.4	65
23	CO2 adsorption by PAMAM dendrimers: Significant effect of impregnation into SBA-15. Microporous and Mesoporous Materials, 2009, 123, 140-149.	4.4	57
24	Adsorption of CO2 on mesocellular siliceous foam iteratively functionalized with dendrimers. Adsorption, 2009, 15, 429-437.	3.0	55
25	The spontaneous combustion behavior of some low rank coals and a range of dried products. Fuel, 2009, 88, 1650-1655.	6.4	55
26	Nanoscale Structural Investigation of Cs <sub>2</sub> CO <sub>3</sub> -Doped MgO Sorbent for CO <sub>2</sub> Capture at Moderate Temperature. Journal of Physical Chemistry C, 2013, 117, 17514-17520.	3.1	55
27	Mechanical/thermal dewatering of lignite. Part 4: Physico-chemical properties and pore structure during an acid treatment within the MTE process. Fuel, 2012, 93, 433-442.	6.4	54
28	Thermal Treatment of Algae for Production of Biofuel. Energy & Fuels, 2013, 27, 1926-1950.	5.1	54
29	Structural elucidation of humic acids extracted from Pakistani lignite using spectroscopic and thermal degradative techniques. Fuel Processing Technology, 2011, 92, 983-991.	7.2	51
30	Investigation of Lignin-water interactions by molecular simulation. Molecular Simulation, 2002, 28, 981-991.	2.0	49
31	Pyrolysis of Mesoporous Silica-Immobilized 1,3-Diphenylpropane. Impact of Pore Confinement and Size. Journal of the American Chemical Society, 2005, 127, 6353-6360.	13.7	48
32	Metal–organic frameworks as stationary phases for mixed-mode separation applications. Chemical Communications, 2014, 50, 3735.	4.1	47
33	An attempt to produce blast furnace coke from Victorian brown coal. Fuel, 2015, 148, 104-111.	6.4	45
34	Pyrolysis—gas chromatography of Australian coals. 1. Victorian brown coal lithotypes. Fuel, 1983, 62, 303-310.	6.4	43
35	Comparison of some physico–chemical properties of Victorian lignite dewatered under non-evaporative conditions. Fuel, 2006, 85, 1987-1991.	6.4	43
36	Selective electrochemical hydrogenation of furfural to 2-methylfuran over a single atom Cu catalyst under mild pH conditions. Green Chemistry, 2021, 23, 3028-3038.	9.0	43

#	Article	IF	CITATIONS
37	CO <sub>2</sub> Capture from Air Using Pelletized Polyethylenimine Impregnated MCF Silica. Industrial & Engineering Chemistry Research, 2019, 58, 3293-3303.	3.7	42
38	Effects of Pretreatment in Steam on the Pyrolysis Behavior of Loy Yang Brown Coal. Energy & Fuels, 2006, 20, 281-286.	5.1	41
39	Ordered micro-porous carbon molecular sieves containing well-dispersed platinum nanoparticles for hydrogen storage. Microporous and Mesoporous Materials, 2009, 119, 39-46.	4.4	41
40	The effect of densification on brown coal physical properties and its spontaneous combustion propensity. Fuel, 2017, 193, 54-64.	6.4	38
41	Charge Equilibration Based on Atomic Ionization in Metal–Organic Frameworks. Journal of Physical Chemistry C, 2015, 119, 456-466.	3.1	37
42	Oxygen Uptake of Tb–CeO <sub>2</sub> : Analysis of Ce <sup>3+</sup> and Oxygen Vacancies. Journal of Physical Chemistry C, 2016, 120, 14382-14389.	3.1	37
43	Desorption Process for Capturing CO <sub>2</sub> from Air with Supported Amine Sorbent. Industrial & Engineering Chemistry Research, 2019, 58, 15606-15618.	3.7	36
44	Water in Brown Coal and Its Removal. , 2004, , 85-133.		35
45	Long time, low temperature pyrolysis of El-Lajjun oil shale. Journal of Analytical and Applied Pyrolysis, 2018, 130, 135-141.	5.5	35
46	Transformation behaviors of C, H, O, N and S in lignite during hydrothermal dewatering process. Fuel, 2019, 236, 228-235.	6.4	35
47	Highly Ordered Hierarchical Mesoporous MnCo <sub>2</sub> O <sub>4</sub> with Cubic <i>l</i> 1±3 <i>d</i> Symmetry for Electrochemical Energy Storage. Journal of Physical Chemistry C, 2016, 120, 23976-23983.	3.1	34
48	Dewatering Low Rank Coals by Mechanical Thermal Expression (MTE) and its Influence on Organic Carbon and Inorganic Removal. Coal Preparation, 2005, 25, 251-267.	0.5	33
49	Molecular modeling of HMS hybrid materials for CO2 adsorption. Fuel Processing Technology, 2005, 86, 1473-1486.	7.2	32
50	Evaluation of several methods of extraction of oil from a Jordanian oil shale. Fuel, 2012, 92, 281-287.	6.4	32
51	Comparison of Physico-Chemical Properties of Various Lignites Treated by Mechanical Thermal Expression. Coal Preparation, 2005, 25, 269-293.	0.5	31
52	Micro-channel development and hydrogen adsorption properties in templated microporous carbons containing platinum nanoparticles. Carbon, 2011, 49, 1305-1317.	10.3	30
53	The impact of water vapor on CO2 separation performance of mixed matrix membranes. Journal of Membrane Science, 2015, 492, 471-477.	8.2	29
54	Coordination polymers from a highly flexible alkyldiamine-derived ligand: structure, magnetism and gas adsorption studies. Dalton Transactions, 2015, 44, 17494-17507.	3.3	29

ALAN L CHAFFEE

#	Article	IF	CITATIONS
55	The effect of densification with NaOH on brown coal thermal oxidation behaviour and structure. Fuel, 2018, 216, 548-558.	6.4	29
56	Mesoporous Silica SBA-15 Supported Co3O4 Nanorods as Efficient Liquid Phase Oxidative Catalysts. Topics in Catalysis, 2012, 55, 571-579.	2.8	28
57	Correlations between Oxygen Uptake and Vacancy Concentration in Pr-Doped CeO <sub>2</sub> . ACS Omega, 2017, 2, 2544-2551.	3.5	28
58	Sulfur Poisoning of Fischer-Tropsch Synthesis Catalysts in a Fixed-Bed Reactor. Applied Catalysis, 1989, 47, 253-276.	0.8	27
59	Amine-functionalised mesoporous silicas as CO2 adsorbents. Studies in Surface Science and Catalysis, 2005, , 887-896.	1.5	27
60	Comparison of Conventional and HF-Free-Synthesized MIL-101 for CO <sub>2</sub> Adsorption Separation and Their Water Stabilities. Energy & Fuels, 2013, 27, 7612-7618.	5.1	26
61	Molecular dynamics simulations on scattering of single Ar, N2, and CO2 molecules on realistic surfaces. Computers and Fluids, 2014, 97, 31-39.	2.5	26
62	Aliphatic components of Victorian brown coal lithotypes. Organic Geochemistry, 1985, 8, 349-365.	1.8	25
63	Attempts to produce blast furnace coke from Victorian brown coal. 2. Hot briquetting, air curing and higher carbonization temperature. Fuel, 2016, 173, 268-276.	6.4	25
64	Separation and analysis of maceral concentrates from Victorian brown coal. Fuel, 2019, 242, 232-242.	6.4	25
65	Lignite–water interactions studied by phase transition—differential scanning calorimetry. Fuel, 2005, 84, 1557-1557.	6.4	24
66	Multidimensional and comprehensive two-dimensional gas chromatography of dichloromethane soluble products from a high sulfur Jordanian oil shale. Talanta, 2014, 120, 55-63.	5.5	24
67	Evaluation of methods for monitoring MEA degradation during pilot scale post-combustion capture of CO2. International Journal of Greenhouse Gas Control, 2015, 39, 407-419.	4.6	24
68	A comparison of adsorption isotherms using different techniques for a range of raw, water- and acid-washed lignites. Fuel, 2006, 85, 1559-1565.	6.4	23
69	Evaluation of comprehensive two-dimensional gas chromatography with flame photometric detection: Potential application for sulfur speciation in shale oil. Analytica Chimica Acta, 2013, 803, 174-180.	5.4	23
70	A comparison of the structure and reactivity of five Jordanian oil shales from different locations. Fuel, 2014, 119, 313-322.	6.4	23
71	Modulating Porosity through Conformer-Dependent Hydrogen Bonding in Copper(II) Coordination Polymers. Crystal Growth and Design, 2015, 15, 3417-3425.	3.0	23
72	Monoethanolamine Degradation during Pilot-Scale Post-combustion Capture of CO <sub>2</sub> from a Brown Coal-Fired Power Station Energy & amp: Fuels 2015, 29, 7441-7455	5.1	23

ALAN L CHAFFEE

#	Article	IF	CITATIONS
73	Hydrogen storage capacity of selected activated carbon electrodes made from brown coal. International Journal of Hydrogen Energy, 2016, 41, 23099-23108.	7.1	23
74	Elevated amyloidoses of human IAPP and amyloid beta by lipopolysaccharide and their mitigation by carbon quantum dots. Nanoscale, 2020, 12, 12317-12328.	5.6	23
75	The effect of cation content of some raw and ion-exchanged Victorian lignites on their equilibrium moisture content and surface area. Fuel, 2007, 86, 2890-2897.	6.4	22
76	The structure and reactivity of a low-sulfur lacustrine oil shale (Colorado U.S.A.) compared with those of a high-sulfur marine oil shale (Julia Creek, Queensland, Australia). Fuel Processing Technology, 2015, 135, 91-98.	7.2	22
77	Study on the Relationship Between Pore Structure and Water Forms in Pore Using Partially Gasified Lignite Char. Energy & Fuels, 2016, 30, 8875-8885.	5.1	22
78	Pyrolysis-GC/MS analysis of biomass and the bio-oils produced from CO/H 2 O reactions. Journal of Analytical and Applied Pyrolysis, 2016, 120, 154-164.	5.5	22
79	Utilization of raw and dried Victorian brown coal in the adsorption of model dyes from solution. Journal of Water Process Engineering, 2017, 15, 43-48.	5.6	22
80	Remediation of mechanical thermal expression product waters using raw Latrobe Valley brown coals as adsorbents. Fuel, 2007, 86, 1130-1138.	6.4	21
81	Impact of preparation methods on SBA-15 supported low cobalt-content composites: Structure and catalytic activity. Journal of Molecular Catalysis A, 2013, 377, 115-122.	4.8	21
82	Pressurized thermal and hydrothermal decomposition of algae, wood chip residue, and grape marc: A comparative study. Biomass and Bioenergy, 2015, 76, 141-157.	5.7	21
83	A Multifunctional, Chargeâ€Neutral, Chiral Octahedral M <sub>12</sub> L <sub>12</sub> Cage. Chemistry - A European Journal, 2019, 25, 8489-8493.	3.3	21
84	The conversion of brown coal to a dense, dry, hard material. Fuel Processing Technology, 1989, 21, 209-221.	7.2	20
85	Confinement effects on product selectivity in the pyrolysis of phenethyl phenyl ether in mesoporous silica. Chemical Communications, 2007, , 52-54.	4.1	20
86	Modeling gas separation in metal-organic frameworks. Adsorption, 2011, 17, 255-264.	3.0	20
87	Comparison of the yields and structure of fuels derived from freshwater algae (torbanite) and marine algae (El-Lajjun oil shale). Fuel, 2013, 105, 83-89.	6.4	20
88	High solubility of Victorian brown coal in â€~distillable' ionic liquid DIMCARB. Fuel, 2015, 158, 23-34.	6.4	20
89	Effect of temperature on the solubility of Victorian brown coal in the ionic liquid DIMCARB. Fuel, 2018, 216, 752-759.	6.4	20
90	A comparison of the NaOH-HCl and HCl-HF methods of extracting kerogen from two different marine oil shales. Fuel, 2019, 236, 880-889.	6.4	20

#	Article	IF	CITATIONS
91	Study on combustion performance of hydrothermally dewatered lignite by thermal analysis technique. Fuel, 2021, 285, 119217.	6.4	20
92	Pyrolysis—gas chromatography of Australian coals. 2. Bituminous coals. Fuel, 1983, 62, 311-316.	6.4	19
93	Studies related to the structure and reactivity of coals. Fuel, 1989, 68, 1538-1543.	6.4	19
94	High-Connectivity Approach to a Hydrolytically Stable Metal–Organic Framework for CO <sub>2</sub> Capture from Flue Gas. Chemistry of Materials, 2018, 30, 6614-6618.	6.7	19
95	MTE water remediation using Loy Yang brown coal as a filter bed adsorbent. Fuel, 2008, 87, 894-904.	6.4	18
96	The remediation of MTE water by combined anaerobic digestion and chemical treatment. Fuel, 2009, 88, 1786-1792.	6.4	18
97	SBA-15 supported cobalt oxide species: Synthesis, morphology and catalytic oxidation of cyclohexanol using TBHP. Journal of Molecular Catalysis A, 2013, 379, 277-286.	4.8	18
98	Coordination Chemistry and Structural Dynamics of a Long and Flexible Piperazine-Derived Ligand. Inorganic Chemistry, 2016, 55, 6692-6702.	4.0	18
99	Shaped polyethyleneimine sorbents for CO 2 capture. Microporous and Mesoporous Materials, 2017, 238, 14-18.	4.4	18
100	The effect of densification with alkali hydroxides on brown coal self-heating behaviour and physico-chemical properties. Fuel, 2019, 240, 299-308.	6.4	18
101	Studies related to the structure and reactivity of coals. Fuel, 1990, 69, 764-770.	6.4	16
102	Assessment of the water quality produced from mechanical thermal expression processing of three Latrobe Valley lignites. Fuel, 2006, 85, 1364-1370.	6.4	16
103	Ambient temperature solubilisation of brown coal in ammonium carbamate ionic liquids. Fuel, 2016, 166, 106-115.	6.4	16
104	Long-Time-Period, Low-Temperature Reactions of Green River Oil Shale. Energy & Fuels, 2018, 32, 4808-4822.	5.1	16
105	Energy efficient method of supercritical extraction of oil from oil shale. Energy Conversion and Management, 2022, 252, 115108.	9.2	16
106	Attempts to produce blast furnace coke from Victorian brown coal. 3. Hydrothermally dewatered and acid washed coal as a blast furnace coke precursor. Fuel, 2016, 180, 597-605.	6.4	15
107	Technoeconomic Evaluation of a Process Capturing CO2 Directly from Air. Processes, 2019, 7, 503.	2.8	15
108	Partial Exchange of Fe(III) Montmorillonite with Hexadecyltrimethylammonium Cation Increases Catalytic Activity for Hydrophobic Substrates. Langmuir, 2010, 26, 4258-4265.	3.5	14

#	Article	IF	CITATIONS
109	Cadmium oxide/alkali metal halide mixtures – a potential high capacity sorbent for pre-combustion CO2 capture. Journal of Materials Chemistry A, 2013, 1, 10962.	10.3	14
110	Reactions with CO/H <sub>2</sub> O of Two Marine Algae and Comparison with Reactions under H <sub>2</sub> and N <sub>2</sub> . Energy & Fuels, 2014, 28, 3143-3156.	5.1	14
111	Recovery of shale oil condensate from different oil shales using a flow-through apparatus. Fuel Processing Technology, 2015, 133, 167-172.	7.2	14
112	Dimethoxymethane Production via Catalytic Hydrogenation of Carbon Monoxide in Methanol Media. ACS Sustainable Chemistry and Engineering, 2020, 8, 2081-2092.	6.7	14
113	The Fate of Trace Elements During MTE and HTD Dewatering of Latrobe Valley Brown Coals. Coal Preparation, 2007, 27, 210-229.	0.5	13
114	Chemical Characterization of MEA Degradation in PCC pilot plants operating in Australia. Energy Procedia, 2013, 37, 877-882.	1.8	13
115	Primary sources and accumulation rates of inorganic anions and dissolved metals in a MEA absorbent during PCC at a brown coal-fired power station. International Journal of Greenhouse Gas Control, 2015, 41, 239-248.	4.6	13
116	Aminopropyl-Functionalized Silica CO <sub>2</sub> Adsorbents via Sonochemical Methods. Journal of Chemistry, 2016, 2016, 1-10.	1.9	13
117	Vacancy Generation and Oxygen Uptake in Cu-Doped Pr-CeO <sub>2</sub> Materials using Neutron and in Situ X-ray Diffraction. Inorganic Chemistry, 2016, 55, 12595-12602.	4.0	13
118	A comparison of primary lignite structure as determined by pyrolysis techniques with chemical characteristics determined by other methods. Fuel, 2006, 85, 998-1003.	6.4	12
119	Pyrolysis of Phenethyl Phenyl Ether Tethered in Mesoporous Silica. Effects of Confinement and Surface Spacer Molecules on Product Selectivity. Journal of Organic Chemistry, 2011, 76, 6014-6023.	3.2	12
120	Molecular indicators of diagenesis in lignite diastereomeric configuration of triterpenoid derived aromatic hydrocarbons. Organic Geochemistry, 1990, 15, 485-488.	1.8	11
121	Lignite clean up of magnesium bisulphite pulp mill effluent as a proxy for aqueous discharge from a ligno-cellulosic biorefinery. Biomass and Bioenergy, 2012, 36, 411-418.	5.7	11
122	Biorefinery process water effluent treatments by salt coagulation. Biomass and Bioenergy, 2013, 56, 189-196.	5.7	11
123	Porous Polyrotaxane Coordination Networks Containing Two Distinct Conformers of a Discontinuously Flexible Ligand. Inorganic Chemistry, 2016, 55, 10467-10474.	4.0	11
124	A comparison of acid treatment in the dewatering of Chinese and Australian lignites by mechanical thermal expression at high temperatures. Fuel Processing Technology, 2016, 144, 282-289.	7.2	11
125	Characterisation of the products of low temperature pyrolysis of Victorian brown coal in a semi-continuous/flow through system. Fuel, 2018, 234, 1422-1430.	6.4	11
126	Ru-zirconia catalyst derived from MIL140C for carbon dioxide conversion to methane. Catalysis Today, 2021, 371, 120-133.	4.4	11

#	Article	IF	CITATIONS
127	Colouring matters of Australian plants. XXIV. Haemofluorone B : New synthetic models and a revised structure. Australian Journal of Chemistry, 1981, 34, 587.	0.9	10
128	THE INFLUENCE OF WATER QUALITY ON THE REUSE OF LIGNITE-DERIVED WATERS IN THE LATROBE VALLEY, AUSTRALIA. Coal Preparation, 2005, 25, 47-66.	0.5	10
129	Investigation of the capacity decay of a CdO–Nal mixed sorbent for pre-combustion CO <sub>2</sub> capture. Journal of Materials Chemistry A, 2015, 3, 5162-5175.	10.3	10
130	Structural Characteristics of Low-Aromaticity Marine and Lacustrine Oil Shales and their NaOH-HCl Kerogens Determined Using 13C NMR and XPS. Australian Journal of Chemistry, 2020, 73, 1237.	0.9	10
131	Microreactor for postcolumn reaction gas chromatography/mass spectrometry with fused silica capillary columns. Analytical Chemistry, 1985, 57, 2429-2430.	6.5	9
132	Modeling gas adsorption in metal organic frameworks. Energy Procedia, 2009, 1, 1273-1280.	1.8	9
133	Silica/Polyethyleneimine Composite Adsorbent S-PEI for CO2Capture by Vacuum Swing Adsorption (VSA). ACS Symposium Series, 2012, , 177-205.	0.5	9
134	Quantification of Aqueous Monoethanolamine Concentration by Gas Chromatography for Postcombustion Capture of CO <sub>2</sub> . Industrial & Engineering Chemistry Research, 2014, 53, 4805-4811.	3.7	9
135	Structural chemistry and selective CO <sub>2</sub> uptake of a piperazine-derived porous coordination polymer. CrystEngComm, 2015, 17, 2196-2203.	2.6	9
136	Cu-Enhanced Surface Defects and Lattice Mobility of Pr-CeO <sub>2</sub> Mixed Oxides. Journal of Physical Chemistry C, 2016, 120, 27996-28008.	3.1	9
137	UV-induced colour generation of pulp and paper mill effluents as a proxy of ligno-cellulosic biorefinery wastewater. Journal of Water Process Engineering, 2019, 29, 100781.	5.6	9
138	Upgrading Microalgal Biocrude Using NiMo/Al-SBA-15 as a Catalyst. Energy & Fuels, 2020, 34, 4618-4631.	5.1	9
139	Pyrolysis of fast growing wood Macaranga gigantea: Product characterisation and kinetic study. Fuel, 2022, 315, 123182.	6.4	9
140	Fast atom bombardment mass spectrometry of seryl- and O-phosphoseryl-containing peptides. Tetrahedron Letters, 1986, 27, 4791-4794.	1.4	8
141	Gas binding to Au13, Au12Pd, and Au11Pd2 nanoclusters in the context of catalytic oxidation and reduction reactions. Journal of Chemical Physics, 2008, 129, 164712.	3.0	8
142	PEI modified mesocellular siliceous foam: A novel sorbent for CO2. Energy Procedia, 2011, 4, 839-843.	1.8	8
143	Improvements in the Pre-Combustion Carbon Dioxide Sorption Capacity of a Magnesium Oxide–Cesium Carbonate Sorbent. Energy & Fuels, 2014, 28, 5284-5295.	5.1	8
144	Improvement in liquid fuel product quality from reactions of grape marc with CO/H2O. Fuel, 2015, 159, 234-240.	6.4	8

#	Article	IF	CITATIONS
145	Effect of Syngas Constituents on CdO- and MgO-Based Sorbents for Pre-combustion CO2 Capture. Energy & Fuels, 2015, 29, 5909-5918.	5.1	8
146	The koËlbel-engelhardt reaction over a silica supported nickel catalyst. Variation of product distributions with reaction conditions. Applied Catalysis, 1986, 26, 123-139.	0.8	7
147	Comparison of the structure and reactivity of a Kansk-Achinsk basin (USSR) coal with those of a Latrobe Valley (Australia) coal. Energy & Fuels, 1990, 4, 28-33.	5.1	7
148	Structural characterisation of Middle Jurassic, high-volatile bituminous Walloon Subgroup coals and correlation with the coal seam gas content. Fuel, 2010, 89, 3241-3249.	6.4	7
149	Multiple sorption cycles evaluation of cadmium oxide–alkali metal halide mixtures for pre-combustion CO <sub>2</sub> capture. Journal of Materials Chemistry A, 2014, 2, 4299-4308.	10.3	7
150	Attempts to produce blast furnace coke from Victorian brown coal. 4. Low surface area char from alkali treated brown coal. Fuel, 2016, 186, 320-327.	6.4	7
151	Atomistic Mechanisms of Thermal Transformation in a Zr-Metal Organic Framework, MIL-140C. Journal of Physical Chemistry Letters, 2021, 12, 177-184.	4.6	7
152	A comparison of the thermal conversion behaviour of marine kerogens isolated from oil shales by NaOH-HCl and HCl-HF methods. Journal of Analytical and Applied Pyrolysis, 2021, 155, 105023.	5.5	7
153	Detailed gas chromatography/mass spectrometric structural determination of olefin oligomerization products. Industrial & Engineering Chemistry Research, 1987, 26, 1822-1824.	3.7	6
154	A simple explanation for the [MH-90]+ ion in the fast atom bombardment mass spectrum of Nα-(t-butyloxycarbonyl)-O-(dibenzylphosphoro)-L-serine. Organic Mass Spectrometry, 1988, 23, 680-683.	1.3	6
155	Studies related to the structure and reactivity of coals. Fuel, 1989, 68, 1549-1557.	6.4	6
156	Fischer-tropsch catalysts derived from surface confined [HnFeCo3(CO)12]nâ^'1 (n = 0, 1). Polyhedron, 1990, 9, 2815-2822.	2.2	6
157	Simulations of model metal-organic frameworks for the separation of carbon dioxide. Energy Procedia, 2011, 4, 568-575.	1.8	6
158	Thermo-chemical reactions of algae, grape marc and wood chips using a semi-continuous/flow-through system. Fuel, 2015, 158, 927-936.	6.4	6
159	Coordination polymers from a flexible alkyldiamine-derived ligand. CrystEngComm, 2017, 19, 5137-5145.	2.6	6
160	Shaped Silica-polyethyleneimine Composite Sorbents for CO2 Capture via Adsorption. Energy Procedia, 2017, 114, 2219-2227.	1.8	5
161	Metal nanoparticles formed by thermal transformation of M-MIL140C (M=In, Rh, Pd). Microporous and Mesoporous Materials, 2021, 324, 111264.	4.4	5
162	Rh/ZrO2@C(MIL) catalytic activity and TEM images. CO2 conversion performance and structural systematic evaluation of novel catalysts derived from Zr-MOF metallated with Ru, Rh, Pd or In. Microporous and Mesoporous Materials, 2022, 336, 111855.	4.4	5

#	Article	IF	CITATIONS
163	Aromatic hydrocarbons from the kolbel-engelhardt reaction. Applied Catalysis, 1985, 19, 419-422.	0.8	4
164	Phase and morphological segregation in Ti-MCM-41. Microporous and Mesoporous Materials, 2012, 151, 466-473.	4.4	4
165	Characterisation of the phase-transformation behaviour of Ce <sub>2</sub> O(CO <sub>3</sub> ) <sub>2</sub> ·H <sub>2</sub> O clusters synthesised from Ce(NO <sub>3</sub> ) <sub>3</sub> ÷6H <sub>2</sub> O and urea. Powder Diffraction, 2014, 29, S84-S88.	0.2	4
166	Formation of a non-porous cobalt-phosphonate framework by small pH change in the preparation of the microporous STA-16(Co). CrystEngComm, 2014, 16, 6296-6299.	2.6	4
167	ISOLATION OF ORGANIC MATTER BY THE NAOH-HCL METHOD FROM TWO MARINE OIL SHALES USING OVEN AND SEALED AUTOCLAVE TECHNIQUES. Oil Shale, 2019, 36, 197.	1.0	4
168	Reducing Greenhouse Emissions from Lignite Power Generation by Improving Current Drying Technologies. , 2002, , 175-187.		4
169	Comparative electron impact, chemical ionization and fast atom bombardment mass spectra of Nα -(t-butyloxycarbonyl)-O-(di-t-butylphosphoro)-L-serine. Organic Mass Spectrometry, 1988, 23, 797-799.	1.3	3
170	Fast Atom Bombardment Mass Spectra of Some N-α-(t-Butoxycarbonyl)-O-(diorganylphosphono)-L-serines and O-(Diorganylphosphono)seryl-Containing Dipeptides and Tripeptides. Australian Journal of Chemistry, 1994, 47, 229.	0.9	3
171	Solvation behaviour and micro-phase structure of formaldehyde-methanol-water mixtures. Journal of Molecular Liquids, 2020, 301, 112444.	4.9	3
172	Characterisation of coal density fractions separated from Victorian brown coal by reflux classification. Fuel, 2021, 292, 120385.	6.4	3
173	Understanding Brown Coal-Water Interactions to Reduce Carbon Dioxide Emissions. , 2002, , 203-216.		3
174	Highly Connected Framework Materials from Flexible Tetra-Isophthalate Ligands. CrystEngComm, 0, , .	2.6	3
175	Improved Methanol Decomposition Catalyst. Studies in Surface Science and Catalysis, 1994, 81, 405-407.	1.5	2
176	The analysis of multiple O-phosphoseryl-containing peptides by fast atom bombardment mass spectrometry. International Journal of Peptide Research and Therapeutics, 1996, 2, 345-351.	0.1	2
177	Molecular dynamics modelling of tethered organics in confined spaces. Molecular Simulation, 2011, 37, 1266-1275.	2.0	2
178	Selective CO2 uptake and vapor adsorption study within Sn(iv) porphyrin crystals. CrystEngComm, 2016, 18, 1515-1522.	2.6	2
179	An adsorption study on STA-16(Co). Microporous and Mesoporous Materials, 2016, 222, 169-177.	4.4	2
180	A versatile modelling approach to determine the hydrophobicity of peptides at the atomic level. Molecular Simulation, 2016, 42, 257-269.	2.0	2

#	Article	IF	CITATIONS
181	Catalytic hydropyrolysis of El-Lajjun and Julia Creek shale oils using flow-through and sealed autoclaves. Journal of Analytical and Applied Pyrolysis, 2019, 143, 104682.	5.5	2
182	Pyrolysis-GC/MS Analysis of Fast Growing Wood Macaranga Species. Indonesian Journal of Science and Technology, 2021, 6, 141-158.	1.5	2
183	Comparison of sample preparation methods for the GCâ¿¿MS analysis of monoethanolamine (MEA) degradation products generated during post-combustion capture of CO 2. International Journal of Greenhouse Gas Control, 2016, 52, 201-214.	4.6	1
184	Thermochemical Reactions of Blue Gum and Fossil Wood with CO/H2O: Some Mechanistic Comments. Energy & Fuels, 2016, , .	5.1	1
185	CO <sub>2</sub> adsorption on SBA-15: A molecular modelling. IOP Conference Series: Earth and Environmental Science, 2018, 144, 012045.	0.3	1
186	<i>p</i> -Xylylenediamine derived ligands as flexible connectors in the design of porous coordination polymers. CrystEngComm, 2019, 21, 3074-3085.	2.6	1
187	Surfactant-controlled crystal growth of metal–organic frameworks and their nanoparticle pyrolysis products. Materialia, 2020, 13, 100849.	2.7	1
188	Novel Adsorption Process Technologies for CO2 Post Combustion Capture Via Amine Type Adsorbents. SSRN Electronic Journal, 0, , .	0.4	1
189	Mesoporous Silica Supported Polyethyleneimine for CO2 Capture from Air. SSRN Electronic Journal, 0,	0.4	1
190	Molecular Clustering in Formaldehyde–Methanol–Water Mixtures Revealed by High-Intensity, High-q Small-Angle Neutron Scattering. Journal of Physical Chemistry Letters, 2021, 12, 480-486.	4.6	1
191	Air Separation For Off-Shore Gas Conversion. Studies in Surface Science and Catalysis, 1994, 81, 555-560.	1.5	0
192	A study on the atomic hydrophobicity of peptides in aqueous solutions using molecular dynamics modeling methods. Proceedings of SPIE, 2008, , .	0.8	0
193	Oxygen uptake, selectivity and reversibility of Tb–CeO2 mixed oxides for air separation. Adsorption, 2017, 23, 465-475.	3.0	0
194	Catalytic hydrotreating of bio-oil derived from Chlorococcum sp IOP Conference Series: Earth and Environmental Science, 2018, 144, 012037.	0.3	0